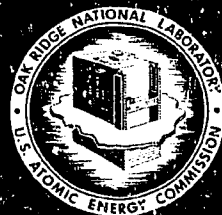


**CALCULATED PHYSICAL AND
BIOLOGICAL RESULTS WHEN NEGATIVELY
CHARGED PIONS ARE USED TO IRRADIATE
A SMALL AND A LARGE "TUMOR" VOLUME
IN A TISSUE PHANTOM**

R. T. Santoro

R. G. Alsmiller, Jr.



OAK RIDGE NATIONAL LABORATORY
OPERATED BY UNION CARBIDE CORPORATION • FOR THE U.S. ATOMIC ENERGY COMMISSION

Contract No. W-7405-eng-26

ORNL-TM-4490

Neutron Physics Division

CALCULATED PHYSICAL AND BIOLOGICAL RESULTS WHEN NEGATIVELY CHARGED
PIONS ARE USED TO IRRADIATE A SMALL AND A LARGE
"TUMOR" VOLUME IN A TISSUE PHANTOM

R. T. Santoro and R. G. Alsmiller, Jr.

MARCH 1974

NOTICE

This report was prepared as an account of work sponsored by the United States Government. Neither the United States nor the United States Atomic Energy Commission, nor any of their employees, nor any of their contractors, subcontractors, or their employees, makes any warranty, express or implied, or assumes any legal liability or responsibility for the accuracy, completeness or usefulness of any information, apparatus, product or process disclosed, or represents that its use would not infringe privately owned rights.

Note:

This work was funded by the
NATIONAL SCIENCE FOUNDATION
under Order NSF/RANN AG-399

NOTICE This document contains information of a preliminary nature and was prepared primarily for internal use at the Oak Ridge National Laboratory. It is subject to revision or correction and therefore does not represent a final report.

OAK RIDGE NATIONAL LABORATORY
Oak Ridge, Tennessee, 37830
operated by
UNION CARBIDE CORPORATION
for the
U. S. ATOMIC ENERGY COMMISSION

MASTER

DISTRIBUTION OF THIS DOCUMENT IS UNLIMITED.

QG

Abstract

The calculated absorbed doses, LET spectra, cell-survival probabilities, oxygen enhancement ratios, and relative biological effectiveness are presented and compared for two negatively charged pion beams, each incident on a 30-cm-thick tissue phantom. All of the biological results were obtained using the cell-inactivation model of Katz *et al.* and parameters for T-1 human kidney cells. The beam parameters were chosen to produce an approximately uniform absorbed dose in a small (2 cm in depth and 1 cm in radius) and in a large (5 cm in depth and 2.5 cm in radius) cylindrical tissue volume, each centered about a depth of 15 cm in the phantom.

1. INTRODUCTION

In a previous paper (Alsmiller, Santoro, Armstrong, Barish, Chandler and Chapman 1973), hereinafter referred to as paper 1, calculated results were presented and compared for the absorbed doses, LET spectra, cell-survival probabilities, oxygen enhancement ratios (OER's), and relative biological effectiveness values (RBE's) when photons, neutrons, negatively charged pions, protons, and alpha particles were incident on a 30-cm-thick tissue phantom. The beam parameters for each type of incident particle were chosen to be approximately those appropriate for single-port irradiation of a cylindrical volume 2 cm in depth and 1 cm in radius centered about a depth of 15 cm in the tissue phantom. In this paper, similar results are presented for an incident pion beam with parameters chosen to be approximately those appropriate to single-port irradiation of a cylindrical volume 5 cm in depth and 2.5 cm in radius centered about a depth of 15 cm in the phantom. With the exception of the energy distribution of the incident pions, the irradiation conditions are similar to those considered by Armstrong and Chandler (1973). The results presented here are compared with the results for incident pions given in paper 1.

Some details of the calculations are given in sec. 2 and the results are discussed in sec. 3.

2. THE CALCULATIONS

The geometry considered is similar to that used for incident pions in paper 1. The pions are assumed to be normally incident on a 30-cm-thick tissue slab. The composition of tissue is the same as that used in paper 1. The incident pion beam is assumed to be uniform over a circular area of 1 cm in radius for the case taken from paper 1 and of 2.5 cm in radius for the second case considered here. As before, the incident pion beams were assumed to be free of contamination.

The energy distributions used for the two cases are shown in fig. 1. The energy distribution shown in fig. 1 as (a) was determined to produce an approximately uniform absorbed dose over the depth interval of 14 to 16 cm in the tissue phantom and the energy distribution shown in fig. 1 as (b) was determined to produce an approximately uniform absorbed dose over the depth interval of 12.5 to 17.5 cm. The numerical procedure used to produce these energy distributions is described elsewhere (Armstrong, Alsmiller and Chandler 1973).

All of the results presented here were obtained with the three-dimensional nucleon-pion transport code HETC (Chandler and Armstrong 1972), as described in paper 1 and elsewhere (Armstrong and Chandler 1973). The cell-survival probabilities, OER's, and RBE's were obtained using the cell-inactivation model of Katz *et al.* (Katz, Ackerson, Homayoonfar and Sharma 1971; Katz, Sharma and Homayoonfar 1972; Katz and Sharma 1973) and the inactivation parameters for T-1 human kidney cells.

BLANK PAGE

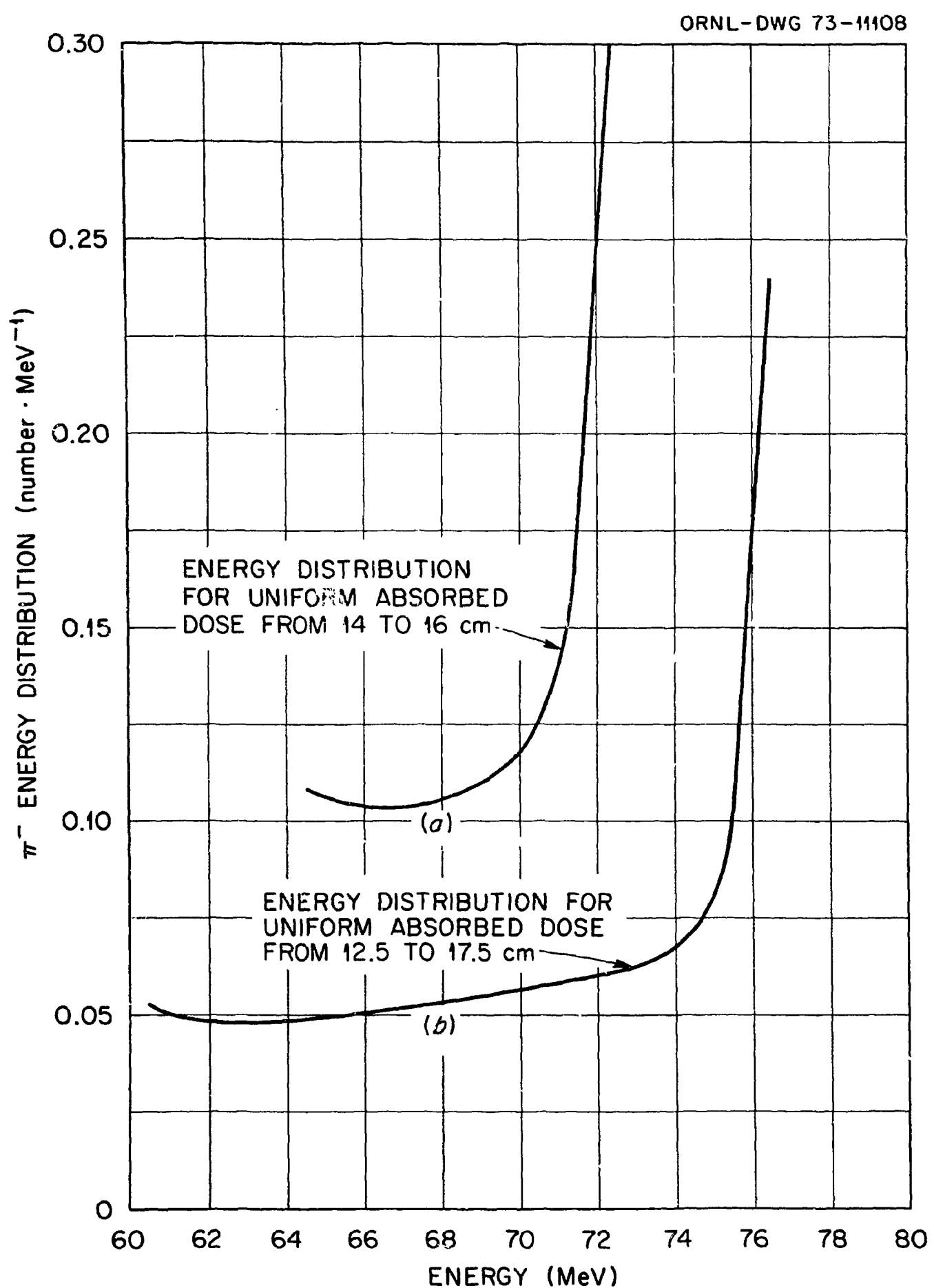


Fig. 1. Energy distributions of incident negatively charged pions that will produce an approximately uniform absorbed dose in the specified depth intervals in a 30-cm-thick tissue phantom. Both distributions are normalized to unity.

3. DISCUSSION OF RESULTS

In fig. 2 the absorbed dose is shown as a function of depth in several radial intervals for the two incident beams considered. The results shown for the small (1-cm radius) beam are absolute. The results shown for the large (2.5-cm radius) beam have been normalized to agree with the results from the 1-cm radius beam in the depth interval of 0 to 1 cm and the radial interval of 0 to 1 cm. The absorbed-dose values given in the figure for the large beam geometry become absolute with units of $\text{RAD}(\text{INCIDENT PION})^{-1}$ when multiplied by 0.164.

In the radial interval of 0 to 1 cm, the absorbed dose from the small beam decreases with increasing depth from the surface of the phantom. This decrease is due primarily to multiple Coulomb scattering, as explained in paper 1. In the radial interval of 0 to 2.5 cm, the absorbed dose from the larger beam does not show a similar decrease as a function of depth because the effects of multiple Coulomb scattering are less important.

For the 2.5-cm incident beam in the radial interval of 0 to 2.5 cm, the ratio of the absorbed dose in the vicinity of the maximum to the absorbed dose at the surface is ~ 2 and is just slightly larger than the corresponding ratio in the radial interval of 0 to 1 cm for the small beam. The difference in the ratios for the two beams is due principally to the effects of multiple Coulomb scattering. At depths well beyond the region of the maximum absorbed dose, the large beam gives a somewhat greater absorbed dose than does the narrow beam. In the radial interval just outside of the incident beam radii, i.e., 1 to 2 cm for the narrow beam and 2.5 to 3.5 cm for the broad beam, the increase in the absorbed dose with increasing depth from the surface of the phantom is due primarily to multiple Coulomb

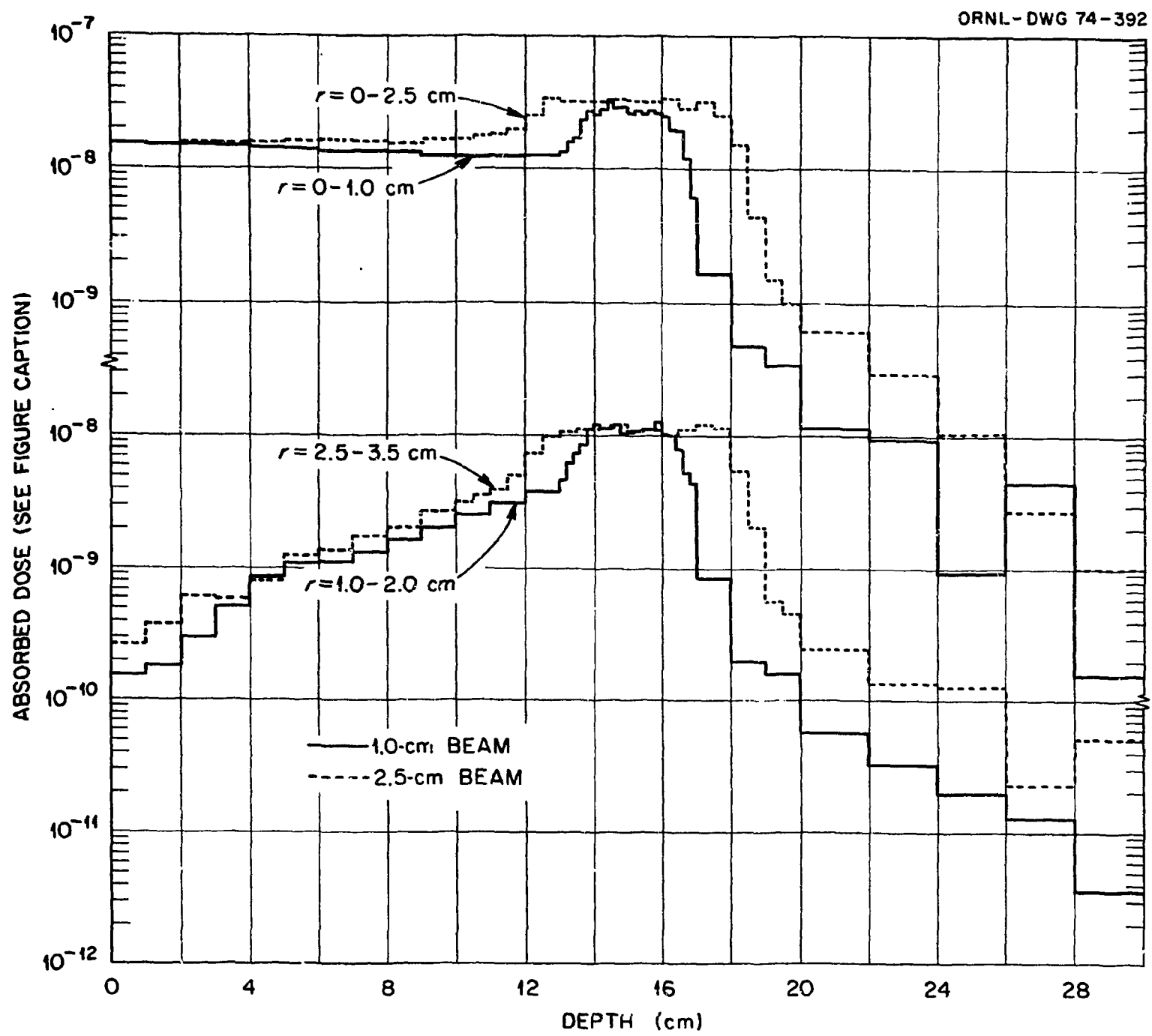


Fig. 2. Absorbed dose vs depth for several radial intervals. The values given for the 1-cm-radius incident beam have units of $\text{RAD}(\text{INCIDENT PION})^{-1}$. The values given for the 2.5-cm-radius incident beam must be multiplied by 0.164 to have units of $\text{RAD}(\text{INCIDENT PION})^{-1}$.

scattering but to some extent is also due to energy deposition by nuclear-reaction products.

LET spectra averaged over the indicated spatial intervals are shown in fig. 3 for the two incident beams. It is to be noted that in fig. 3 the results are presented with an absolute normalization. In the depth interval of 20 to 30 cm, the histogram for the incident 2.5-cm-radius beam is shown for only $\text{LET} < 10^3 \text{ MeV cm}^{-1}$ because in this depth interval adequate statistical accuracy was not obtained in the calculations at the higher LET values. The histograms are shown for only $\text{LET} > 31.6 \text{ MeV cm}^{-1}$, and it is assumed that photons, electrons, and positrons deposit all of their energy at LET values $< 31.6 \text{ MeV cm}^{-1}$. Only a few error bars corresponding to one standard deviation are shown. The abrupt change in the magnitude at specific values of LET (e.g., at $2.5 \times 10^3 \text{ MeV cm}^{-1}$) is due to the fact that some specific type of particle does not contribute at the higher LET values. This fact is borne out in paper 1 and in the work of Armstrong and Chandler (1973) where the contributions of various particle types to the total LET spectra are given. The integral LET spectra, i.e., the fraction of the absorbed dose with $\text{LET} > L$ obtained by integrating the distributions in fig. 2 are shown as a function of L in table 1.

The cell-survival probabilities for aerobic and anoxic T-1 human kidney cells are shown in figs. 4 and 5, respectively, as a function of depth for the two incident pion beam geometries considered. In fig. 4 the cell-survival probability for the small (1-cm radius) beam has been taken to be 0.30 in the depth interval of 0 to 1 cm and in the radial interval of 0 to 1 cm, and the cell-survival probability for the large (2.5-cm radius) beam has been taken to be 0.30 in the depth interval of 0 to 1 cm and in the

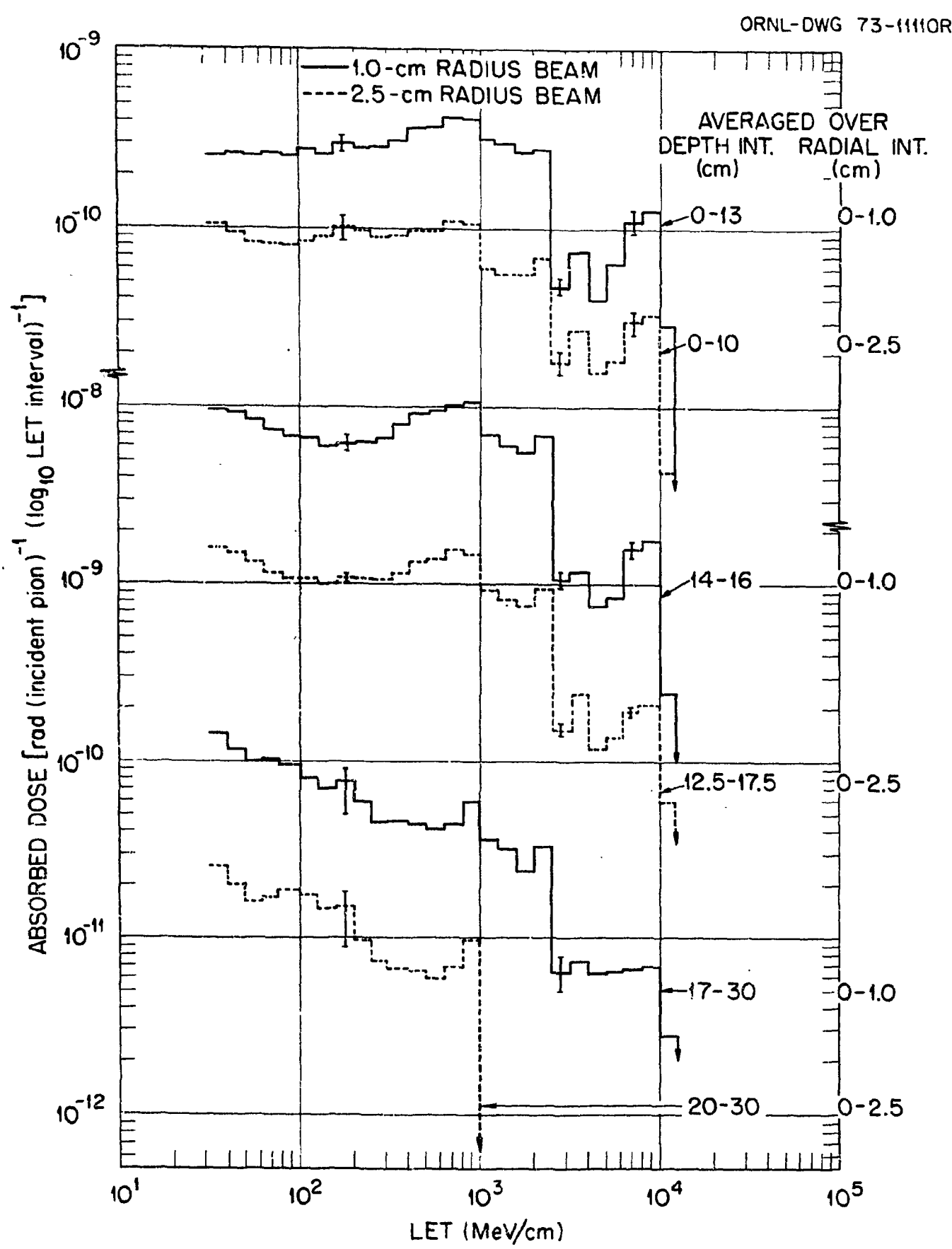
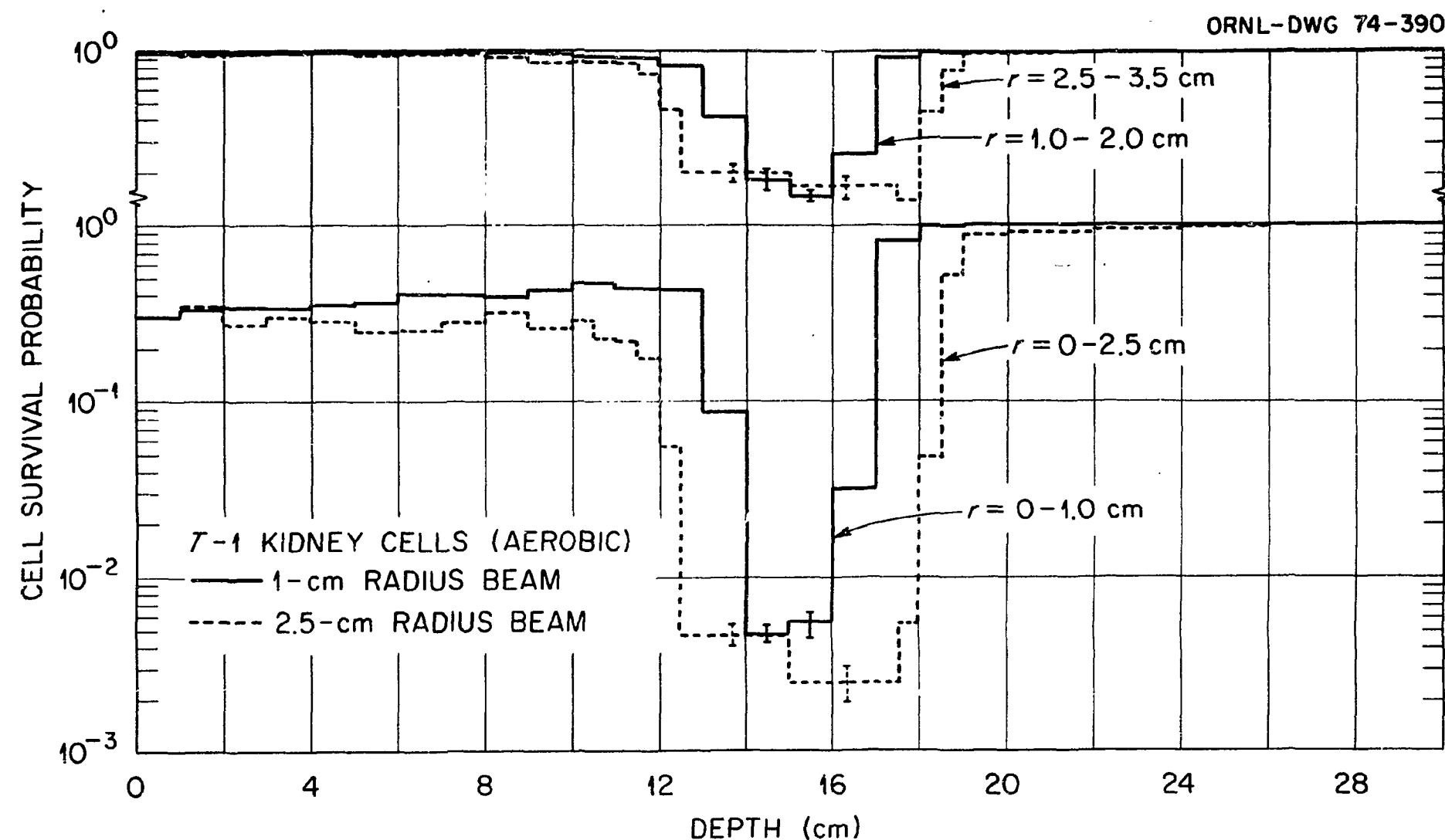


Fig. 3. LET spectra averaged over the indicated spatial intervals.

Table 1. Integral LET Spectra Averaged Over the Indicated Spatial Intervals for the Small and Large Beam Geometries

L (MeV cm ⁻¹)	Fraction of the Absorbed Dose with LET > L					
	1-cm Radius Beam			2.5-cm Radius Beam		
	Depth Interval (cm)					
0-13	14-16	17-30	0-10	12.5-17.5	20-30	
3.16×10^1	.044	.55	.53	.069	.46	.59
1.00×10^2	.035	.40	.30	.052	.33	.31
2.00×10^2	.029	.33	.21	.041	.27	.18
5.01×10^2	.019	.23	.13	.027	.18	.10
1.00×10^3	.011	.12	.071	.015	.091	
1.58×10^3	.0072	.072	.043	.010	.058	
2.51×10^3	.0036	.027	.017	.0056	.024	
3.98×10^3	.0027	.018	.012	.0038	.016	
6.31×10^3	.0019	.013	.0067	.0026	.013	
1.00×10^4	.00020	.00091	.0012	.00016	.0013	



12

Fig. 4. Cell-survival probabilities for aerobic T-1 human kidney cells vs depth for several radial intervals.

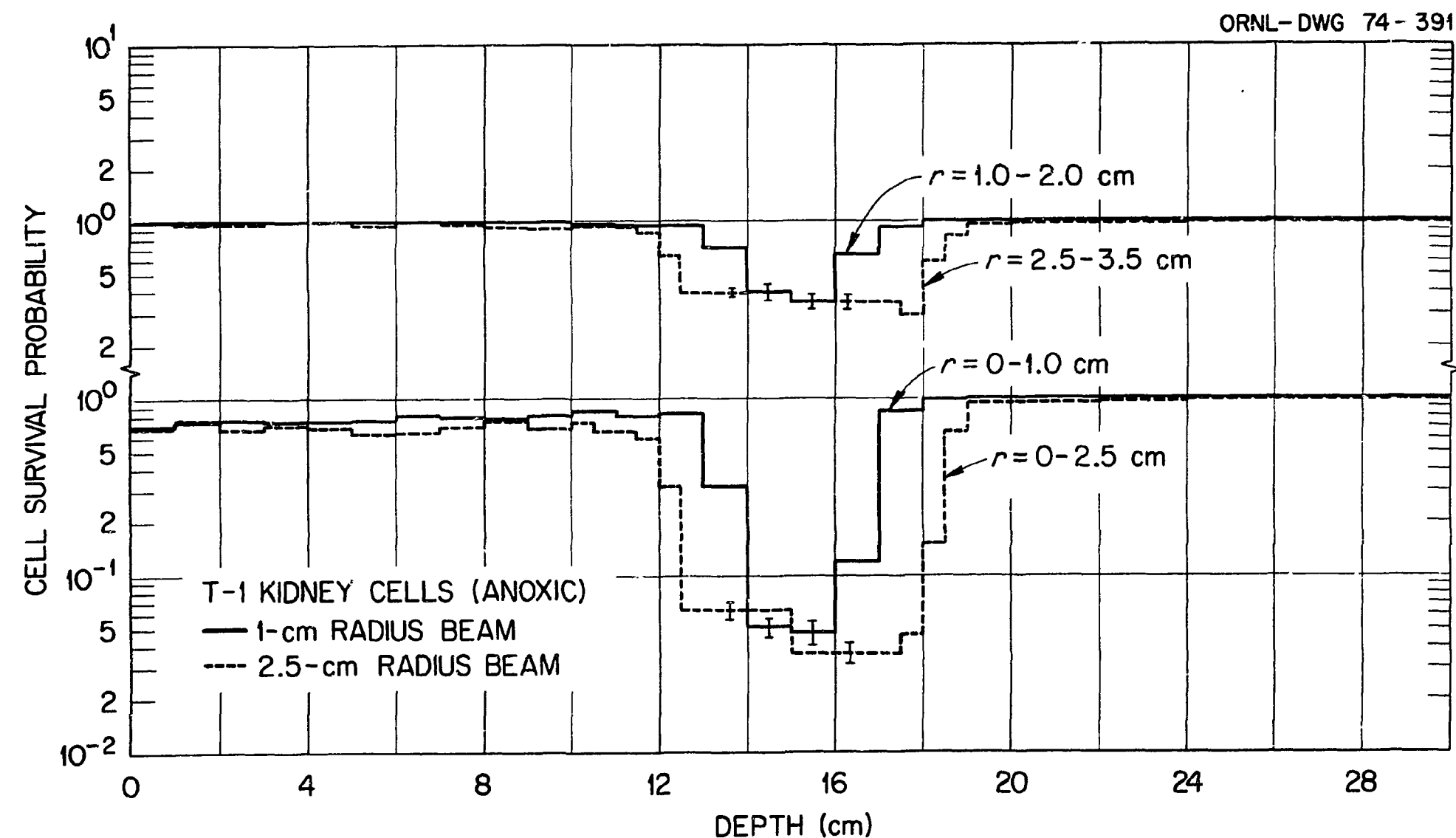


Fig. 5. Cell-survival probabilities for anoxic T-1 human kidney cells vs depth for several radial intervals.

radial interval of 0 to 2.5 cm. In fig. 5 the number of incident pions for each of the beam geometries considered was taken to be the same as that used in fig. 4; that is, the cell-survival probabilities were normalized as described above to obtain the results shown in fig. 4, and this normalization was not changed in obtaining the results in fig. 5. Where shown in figs. 4 and 5, the error bars are statistical and represent one standard deviation.

Note that the 2.5-cm radius beam gives a cell-survival probability comparable to that of the 1-cm-radius beam in the vicinity of the irradiation volume, i.e., in the radial interval of 0 to 2.5 cm and depth interval of 12.5 to 17.5 cm for the large beam and in the radial interval of 0 to 1 cm and depth interval of 14 to 16 cm for the small beam. The difference in the cell-survival probabilities at depths preceding the irradiation volume is probably due to the fact that multiple scattering of the incident pion beam is more significant for the small beam than for the large beam. For the larger radial intervals shown in figs. 4 and 5, the cell-survival probabilities are nearly unity except in the immediate vicinity of the corresponding irradiation volumes of the two incident beams. In the larger radial intervals, the cell-survival probabilities in the 14- to 16-cm depth interval for the 1-cm-radius beam and in the 12.5- to 17.5-cm depth interval for the 2.5-cm-radius beam are comparable.

A comparison of the OER's and RBE's is given in table 2 for the two beam geometries. These data are for a 10% survival level averaged over the indicated spatial intervals. For the spatial intervals considered and within the statistical accuracy of the calculations, the results are comparable for both beam geometries.

Table 2. OER and RBE Values at 10% Survival Level for T-1 Kidney Cells Averaged Over the Indicated Spatial Intervals

Depth (cm)	1-cm-Radius Beam		Depth (cm)	2.5-cm-Radius Beam	
	Radial Interval 0-1 cm	Radial Interval 1-2 cm		Radial Interval 0-2.5 cm	Radial Interval 2.5-3.5 cm
OER			OER		
0-13	2.5	2.4	0-10	2.4	2.1
14-16	1.6	1.8	12.5-17.5	1.7	1.6
17-30	1.6	1.6	20-30	1.7	1.5
RBE Aerobic			RBE Aerobic		
0-13	1.1	1.1	0-10	1.1	1.3
14-16	2.0	1.6	12.5-17.5	1.9	1.9
17-30	1.8	2.0	20-30	1.8	2.2
RBE Anoxic			RBE Anoxic		
0-13	1.2	1.3	0-10	1.2	1.6
14-16	3.4	2.5	12.5-17.5	3.0	3.1
17-30	2.8	3.3	20-30	3.3	4.0

REFERENCES

ALSMILLER, R. G., Jr., SANTORO, R. T., ARMSTRONG, T. W., BARISH, J., CHANDLER, K. C., and CHAPMAN, G. T., 1973, ORNL-TM-4369, Oak Ridge National Laboratory.

ARMSTRONG, T. W., ALSMILLER, R. G., Jr., and CHANDLER, K. C., 1973, ORNL-TM-4078, Oak Ridge National Laboratory.

ARMSTRONG, T. W. and CHANDLER, K. C., 1973, ORNL-TM-4294, Oak Ridge National Laboratory (to be published in Radiat. Res.).

CHANDLER, K. C. and ARMSTRONG, T. W., 1972, ORNL-4744, Oak Ridge National Laboratory.

KATZ, R., ACKERSON, B., HOMAYOONFAR, M., and SHARMA, S. C., 1971, Radiat. Res. 47, 402.

KATZ, R., SHARMA, S. C., and HOMAYOONFAR, M., 1972, The Structure of Particle Tracks. Chapter 6 of Topics in Radiation Dosimetry, Suppl. 1 to Radiation Dosimetry, Ed. Frank A. Attix, Academic Press, New York.

KATZ, Robert, and SHARMA, S. C., 1973, Nucl. Instr. Meth. 111, 93.